Psychophysiology, 50 (2013), 325–333. Wiley Periodicals, Inc. Printed in the USA.

DOI: 10.1111/psyp.12030

Neural correlates of behavioral variation in healthy adults' antisaccade performance

DAVID J. SCHAEFFER,[a] MICHAEL T. AMLUNG,[b] QINGYANG LI,[c] CYNTHIA E. KRAFFT,[b] BENJAMIN P. AUSTIN,[d] KARA A. DYCKMAN,[b] AND JENNIFER E. MCDOWELL[a,b,e]

[a]Department of Neuroscience, University of Georgia, Athens, Georgia, USA
[b]Department of Psychology, University of Georgia, Athens, Georgia, USA
[c]Child Mind Institute, New York, New York, USA
[d]UW Cardiovascular Research Center, University of Wisconsin School of Medicine and Public Health, Madison, Wisconsin, USA
[e]Bio-Imaging Research Center, University of Georgia, Athens, Georgia, USA

Abstract

Cognitive control is required for correct antisaccade performance. High antisaccade error rates characterize certain psychiatric disorders, but can be highly variable, even among healthy groups. Antisaccade data were acquired from a large sample of healthy undergraduates, and error rate was quantified. Participants who reliably made few errors (good, $n = 13$) or many errors (poor, $n = 13$) were recruited back to perform antisaccades during fMRI acquisition. A data-derived model was used to compare signal between good and poor performers during blocks of antisaccade trials. Behaviorally derived regressors were used to compare signal between good and poor performers during correct and error trials. Results show differential activation in middle frontal gyrus and inferior parietal lobule between good and poor performers, suggesting that failure to recruit these top-down control regions corresponds to poor antisaccade performance in healthy young adults.

Descriptors: Functional magnetic resonance imaging (fMRI), Antisaccade, Cognitive control

Saccades support reflexive-like exploration of our environment via rapid redirection of gaze to center the fovea on an object or place of interest (Leigh & Zee, 2006). In daily life, however, goal-directed behavior may require cognitive control to modify reflexive responses. For instance, cognitive control over reflexive saccades can avert gaze from aversive or inappropriate stimuli. As such, evaluating the ability to inhibit reflexive saccades in the face of prepotent stimuli provides a simple and effective index of cognitive control. Antisaccade tasks require the inhibition of a saccade toward a suddenly appearing visual cue and the subsequent generation of a saccade away from the cue (Hallett, 1978). An initial glance towards the cue constitutes an error and may be considered a failure to instate cognitive control. High antisaccade error rates characterize certain psychiatric disorders, but error rates can be highly variable, even among healthy groups (Hutton & Ettinger, 2006). This study sought to (a) identify a subset of healthy participants who, based on antisaccade performance, may have difficulty instating cognitive control, and (b) characterize that deficit in terms of neural circuitry.

Support was provided by National Institute of Mental Health (MH001852), the National Science Foundation Graduate Research Fellowship Program, and the UGA Bio-Imaging Research Center.

Address correspondence to: Jennifer E. McDowell, Department of Psychology, University of Georgia, Athens, GA 30602. E-mail: jemcd@uga.edu

Prosaccades and antisaccades share functional neuroanatomy (for review, see McDowell, Dyckman, Austin, & Clementz, 2008); however, changed levels of activation in the basic saccadic circuitry may be required to support antisaccade performance (Hutton & Ettinger, 2006; Munoz & Everling, 2004). When directly compared with prosaccades, antisaccades show increased activation in posterior parietal cortex (PPC), frontal eye fields (FEF), and supplementary eye fields (SEF; Connolly, Goodale, DeSouza, Menon, & Vilis, 2000; DeSouza, Menon, & Everling, 2002; Dyckman, Camchong, Clementz, & McDowell, 2007).

In addition to differences in the levels of activation within the basic saccadic circuitry, additional regions may be recruited to support the increased cognitive complexity of antisaccade performance. Of the possible regions involved in antisaccade-related cognitive control, PPC and prefrontal cortex (PFC) seem to play a critical role in correct antisaccade performance. Specifically, data from nonhuman primate electrophysiology, human lesion, and human functional neuroimaging studies converge to suggest that regions of PPC are involved in the coordinate transformation required for correct antisaccade performance. Recordings of neural activity in PPC of nonhuman primates during pro- and antisaccades have shown PPC to be active just prior to an antisaccade, suggesting that the PPC encodes the signal to look away from the cue, rather than toward it (Zhang & Barash, 2000). Humans with parietal lobe lesions have displayed impairment in the ability to generate antisaccades, providing further support for the thesis that parietal cortex updates visuomotor space to allow for movements

away from the cue (Sharpe, Cheng, & Eizenman, 2011). Although regions of parietal cortex are important for processing position data for both pro- and antisaccades, functional neuroimaging has shown that, when compared to prosaccades, blood oxygenation level dependent (BOLD) signal during antisaccades is greater in regions of inferior parietal cortex (Connolly et al., 2000; Krafft et al., 2012).

Regions of PFC also have been shown to be involved in correct antisaccade performance. Functional neuroimaging studies comparing pro- and antisaccades have provided evidence that the PFC shows activation during antisaccade trials, but not prosaccade trials (DeSouza et al., 2002; Dyckman et al., 2007). Other studies suggest a more specific timing role of the PFC, such that activation begins before response generation (McDowell et al., 2005), a necessary characteristic for PFC modulation of error avoidance on the antisaccade task. During the period prior to pro- and antisaccades, the dorsolateral PFC (DLPFC) has shown greater activation for antisaccades, suggesting that the DLPFC is involved in the preparation necessary to suppress prosaccades toward the cue (DeSouza et al., 2002). Electrophysiological recordings suggest that singals from the PFC suppress unwanted eye movments by modulating the activity of the FEF and superior colliculous through direct projections to those regions (Johnston & Everling, 2006; Munoz & Everling, 2004). Furthermore, data from electroencephalography (EEG) suggest that prestimulus signals from the PFC modulate correct antisaccade performance by sending top-down signals to visual cortex, which function to complement motor preparation in reducing the propensity to glance toward the cue (Clementz et al., 2010).

Additional information regarding the functional roles of the PPC and PFC has been provided by studies that dissociate patterns of activation between correct and error antisaccade trials. In an event-related functional magnetic resonance imaging (fMRI) study, Curtis and D'Esposito (2003) demonstrated increased levels of activation in PPC and FEF during correct antisaccade performance not present during antisaccade errors or prosaccade trials. Ford, Goltz, Brown, & Everling (2005) compared brain activation during correct and error antisaccade trials and found that activation in frontal and cingulate cortices was associated with correct, but not error antisaccade trials. Taken together, results from the Curtis and Ford studies highlight the requisite role of parietal and frontal activation in correct antisaccade performance.

Although neural deficits associated with poor antisaccade performance have been well documented in clinical populations (for review, see Hutton & Ettinger, 2006), there is a relative dearth of information regarding the neural correlates of poor antisaccade performance in the healthy population. Understanding the neural correlates underlying poor saccadic control within the healthy population may (a) help to identify neural circuitry functioning associated with low levels of cognitive control within nonclinical populations, and (b) serve as an impetus to explore failures of cognitive control in other domains, particularly among people who are vulnerable to these types of failures. In healthy adults, for instance, measures of the antisaccade task performance (e.g., percentage of direction errors) have been shown to correlate with cognitive measures of working memory and intelligence domains (Klein, Rauh, & Biscaldi, 2010).

By acquiring eye movement data from a large sample of healthy undergraduates, the present study sought to identify both good- and poor-performing (based on percent of correct responses) subsets of a healthy sample. Once participants were divided into good- and poor-performing groups, patterns of brain activation corresponding to antisaccade performance were compared. Because poor performers generate a higher proportion of error trials, it was hypothesized that the poor group would show reduced prefrontal (DeSouza et al., 2002; Ford et al., 2005) and parietal (Connolly et al., 2000) activation when compared to the good group. To test for differences between good and poor performers across the blocks of antisaccade trials, a hybrid independent component analysis (ICA; McKeown, 2000) was used. Furthermore, good and poor performers were expected to show differential activation of frontal and parietal regions during correct and error trials (Curtis & D'Esposito, 2003; Ford et al., 2005). The effects of the interaction of Group × Trial Performance were assessed by convolving hemodynamic responses based on correct and error responses separately, then comparing activation patterns correlated with each type of response.

Method

Participants

A large initial sample ($N = 296$, mean age = 19.3 years, $SD = 1.7$; 60.8% female) of right-handed undergraduate students was recruited through the Psychology Research Pool to participate in this study (see Li et al., 2012, for more information). Participants had no history of psychiatric illness or severe head trauma via self-report. Two groups, good performers ($n = 13$) and poor performers ($n = 13$), were selected via performance on screening sessions to perform the antisaccade task in the MRI while eye movements were recorded. One participant from each group was omitted from the final analysis due to excessively noisy eye movement data, resulting in 12 participants in each group (good, mean age = 19.2 years, $SD = 1.2$, 46.1% female; poor, mean age = 19.5 years, $SD = 0.9$, 61.5% female). Groups did not differ on these demographic variables. Participants provided written informed consent and were given course credit or monetary payment for their time. The University of Georgia Institutional Review Board approved this study.

Testing Sessions

Sessions 1 and 2. The present study consisted of two behavioral testing sessions and a fMRI session. During Sessions 1 and 2, participants completed the antisaccade task while their eye movements were recorded at 500 Hz using an infrared-based eye tracking system (Eye Track Model 310; Applied Science Laboratories, Waltham, MA). A chin rest placed participants 70 cm from a flat color monitor and was used to prevent head movements. A block design was used in which seven fixation blocks were alternated with six antisaccade blocks (eight trials per block). On fixation blocks, participants were instructed to stare at a magenta cue (1° diameter) in the center of the screen. On antisaccade trials, a blue cue (1° diameter) was presented in the center of the screen for a random interval between 1,500 ms and 2,000 ms (mean duration = 1,750 ms). The center cue disappeared, and then after a gap of 200 ms, a blue peripheral cue was presented at ± 5° or 10° from fixation on the horizontal plane for 1,250 ms. A 200-ms gap was used because it has been shown to produce more error trials than nongap versions of the task (Fischer, Gezeck, & Hartnegg, 2000). Participants were instructed not to look at the cue when it jumped to the side, and to move their eyes to the opposite side of the screen at the same distance from the center.

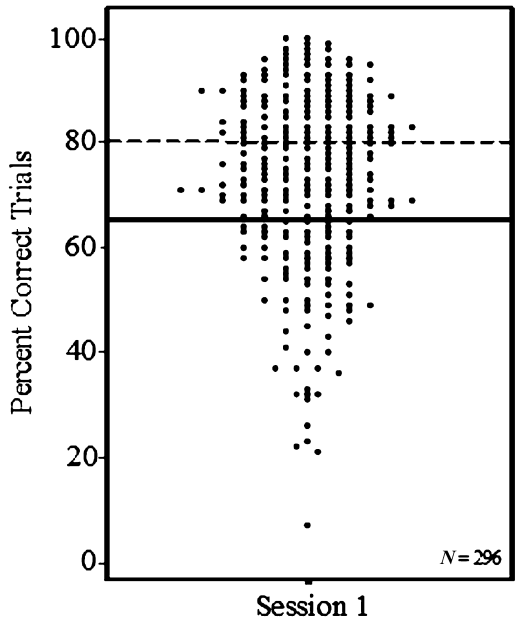

Figure 1. Distribution of percent correct antisaccades from screening session 1 ($N = 296$). Lines represent upper and lower third cutoff points; good performers were defined as scoring above 80% (dashed line) correct and poor performers below 65% (solid line).

Eye movement data were analyzed using MATLAB (The Mathworks Inc., Natick, MA). Trials with blinks during stimulus onset and trials with no saccades were eliminated. Eye movement reaction times within 80 ms of peripheral cue onset were excluded, as the movements were likely not in response to the cue. Saccades were scored for direction, latency, and gain. Trials with antisaccade errors (initial saccades made in the same direction of the cue) were scored for error correction (saccades in the opposite direction after a first movement in the wrong direction).

Participants with correct antisaccade performance in the upper ($\geq$ 80% correct) or lower ($\leq$ 65% correct) thirds of the distribution in Session 1 were invited to return for Session 2 (Figure 1). If a participant's correct antisaccade score in Session 2 remained in the same third of the distribution as it was in Session 1, then performance was considered to be reliable. Participants with reliable performance were invited to Session 3, during which fMRI data were collected while participants were engaged in the antisaccade task.

Session 3. During Session 3, participants completed the antisaccade task in the MRI where functional images and eye movements were recorded simultaneously. fMRI data were acquired using a 3T GE Signa scanner at the University of Georgia Bio-Imaging Research Center. During scanning, heads were stabilized by padding and a forehead strap. Eye movements were recorded using a MR compatible eye tracker (MeyeTrack, SensoMotoric Instruments, Inc., Berlin, Germany). A dual mirror system was mounted 16 mm from the participant's nasion on the head coil; one mirror reflected the image of the participant's eye to an infrared camera placed at the rear of the bore, while a second mirror allowed participants to view a projection screen placed in front of the bore. Eye movements were digitized at 60 Hz and displayed on a computer screen to be monitored by the experimenter during the task. Stimulus presentation was controlled using Presentation software (Neurobehavioral Systems, Albany, CA). The stimuli of Session 3 (Figure 2) were identical to Sessions 1 and 2, apart from a central fixation time fixed at 1,600 ms and the peripheral cue time of 950 ms. Before entering the scanner, participants were instructed not to look at the cue when it jumped to the side, and to move their eyes to the opposite side of the screen at the same distance from the center. Eye movement data were scored for saccade direction to determine correct or error responses on a trial-by-trial basis.

During each scan session, two localizer images were taken to ensure accurate whole brain coverage. T1-weighted structural images were acquired axially using spoiled gradient-recall protocol (.9375 × .9375 × 1.2 mm, 150 slices, TR = 7.8 ms, TE = 3 ms, flip angle = 20°, scan time = 6 min 20 s). For the antisaccade run, T2*-weighted images were acquired using 33 gradient-recalled echo-planar images (EPI; 3.44 × 3.44 × 4 mm, TR = 2,000 ms, TE = 30 ms, flip angle = 90°). To allow for scanner stabilization, four images (8-s scan time) were acquired before the run began; these images were discarded, then image recoding for the functional run began (scan time = 4 min 46 s). The images were

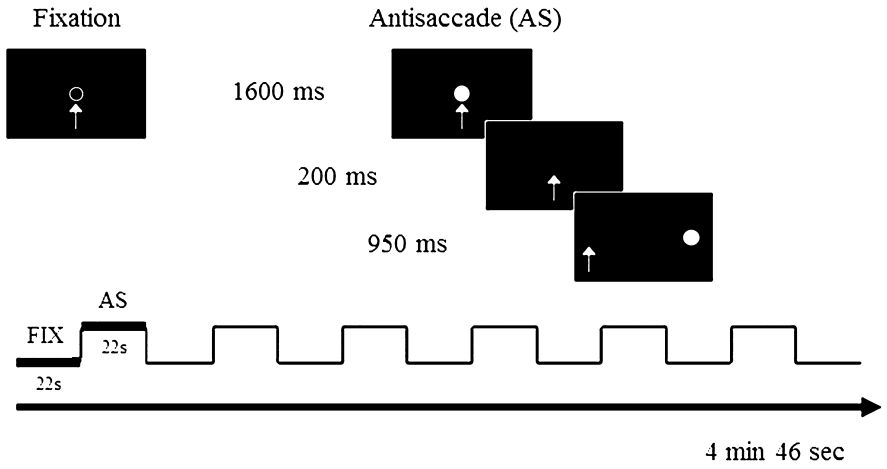

Figure 2. Stimuli and experimental design for fMRI session. The arrow indicates where the participant should look for each stimulus presentation. The run consisted of seven fixation blocks alternated with six blocks consisting of eight antisaccade trials. During the experiment, the fixation and antisaccade cues were presented as magenta and blue, respectively.

collected obliquely, with the slices aligned to the superior margin of the participants' anterior commissure and the inferior margin of the posterior commissure.

Image Analysis

Individual preprocessing. fMRI analyses were conducted using Analysis of Functional NeuroImages (AFNI; Cox, 1996). Functional EPI data processing began with voxelwise despiking of the time series data. For each individual, motion correction was done by registering functional volumes to a base volume, which was identified by the following criteria: the median volume of the longest window of time points with the lowest number of outlier voxels. Functional images were slice-time corrected and aligned to T1-weighted anatomical volumes. Each functional volume was then blurred using a 4-mm full-width at half-maximum (FWHM) Gaussian filter. Functional time series were normalized by dividing the signal at each voxel by the mean signal intensity across the entire time series and multiplying the result by 100.

GLM analyses. This study sought to (a) use a data-derived approach to assess differences between good and poor performers across the blocks of antisaccade trials, and (b) use a behaviorally derived approach to assess differences between good and poor performers on correct and error trials. Thus, two separate GLM analyses were conducted: one data driven and the other behaviorally driven.

Data-derived model. To acquire a model-free task-related regressor for the first GLM analysis, a hybrid ICA was performed similar to the approach developed by McKeown (2000) and implemented in Dyckman et al. (2007). First, all subjects' preprocessed data were transformed into Talaraich space (Talaraich & Tournoux, 1998). Second, an averaged dataset was created for input to FSLs MELODIC (Beckmann & Smith, 2004). The ICA yielded 33 spatially independent components. To avoid under- or overfitting, the number of ICA components was automatically estimated for optimum ICA dimensionality by MELODIC using the Laplace approximation to the Bayesian evidence for the model order. The first component had the same peak frequency as our experimental design and thus was used as a task regressor. Estimates of roll, pitch, and yaw (acquired during motion correction) were used as motion regressors. Estimates of motion were obtained from the output matrix of volume registration, which corresponded to the amount of adjustment to roll, pitch, and yaw (in mm) that was needed to register each volume (i.e., TR) to a base volume. The base volume was chosen by identifying the median volume of the longest window of time points with the lowest number or outlier voxels. Using the coefficients yielded from the ICA-based GLM analysis, group level voxelwise one-sample *t* tests were conducted for the good performers and poor performers to visualize antisaccade task-related BOLD signal change. A voxelwise *t* test between good and poor performers was performed to test between-group differences in BOLD signal change.

Behaviorally derived model. To test for specific trial performance effects, a second analysis was conducted based on individual participant's performance across the task. Eye movement data were scored to identify the response to each trial as either correct or error. Using the time points at which correct or error responses occurred, estimated task-related regressors were created by convolving the responses with the hemodynamic response function. Thus, for each participant, we created a correct regressor and an error regressor. Unscorable trials were not modeled in the regressors. Functional images were then transformed into Talaraich space and resampled to a resolution of $4 \times 4 \times 4$ mm. For each participant, a GLM analysis was conducted using the correct and error-related regressors and the motion regressors discussed in the data-derived model section above. Using the coefficients yielded from the GLM analysis, voxelwise *t* tests between correct and error trials were performed to test for within-group differences in BOLD signal change for good and poor performers. A 2×2 analysis of variance (Group × Trial Performance) was conducted to assess BOLD activation related to correct and error trials for good and poor performers.

To protect against false positives, a clustering method derived from Monte Carlo simulations (accounting for the 4-mm FWHM Gaussian filter and with a connectivity radius of 5.7 mm) was applied to the statistical parametric maps (Ward, 2000). Based on these simulations, the familywise alpha of .05 was preserved with an a priori voxelwise probability of .025 and three-dimensional clusters with a minimum volume of 1,088 µl (17 or more voxels). Data were clustered using AFNI, and resulting statistical parametric maps were used to identify regional BOLD signal changes.

Results

Behavioral Results

The percentage of correct antisaccade trials during Session 2 significantly differed between good (mean = 91.8%, *SD* = 4.5) and poor (mean = 53.6%, *SD* = 7.0) ($t = 13.6$, $p < .05$) performers with usable data from 100% of participants The group difference persisted at Session 3: good (mean = 91.6%, *SD* = 4.0) significantly differed from poor (mean = 60.4%. *SD* = 10.3) ($t = 9.8$, $p < .05$) performers with usable eye movement data available for 92.3% of participants. Both groups corrected antisaccade errors at a high rate (good = 100.0% and poor = 89.6%).

Independent samples *t* tests were conducted to compare reaction times during correct and error trials between good and poor performers. Although reaction times of good performers (mean = 260.2 ms; *SD* = 30.4) were slower than poor performers (mean = 238.4 ms; *SD* = 35.4) during correct trials, differences did not reach significance: $t(22) = 1.6$, $p = .11$. Similarly, during error trials, reaction times of good performers (mean = 201.2 ms; *SD* = 31.4) were slower than poor performers (mean = 176.2 ms; *SD* = 37.9), but differences did not reach significance: $t(22) = 1.6$, $p = .11$. With a much larger sample size, we recently reported (Li et al., 2012) a pattern of good performers showing slower response times in healthy subjects.

Imaging Results

Data-derived model. Clustered one-sample *t* maps comparing BOLD signal change for each group versus zero were calculated (Figure 3). Both groups showed increased BOLD signal change in regions known to be involved in antisaccade performance: SEF, FEF, PPC, frontal cortex, middle occipital gyrus (MOG), striatum, and thalamus. A whole brain, between-groups *t* map showed differences between BOLD signal change in good and poor performers (Table 1). Good performers showed reduced BOLD signal change in left cuneus. Poor performers showed reduced BOLD signal change in right middle frontal gyrus (MFG), bilateral inferior parietal lobule (IPL), left MOG, and left cerebellum.

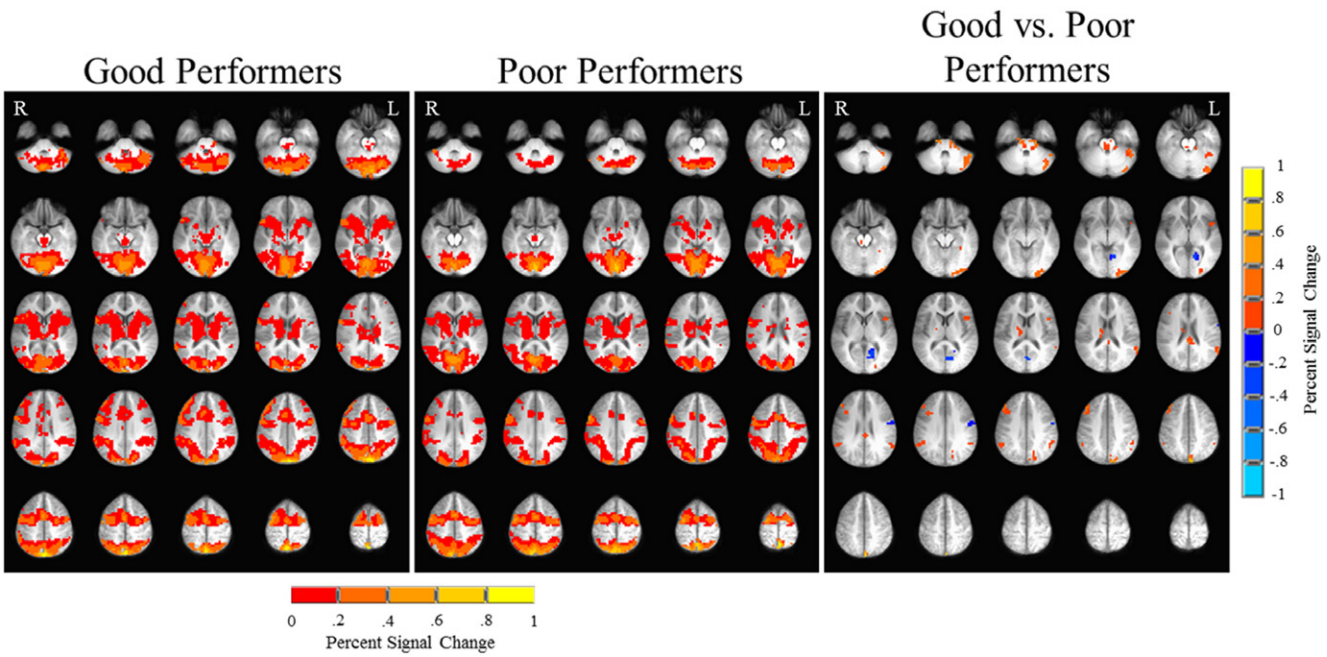

Figure 3. Hybrid independent component analysis. Axial slices ($z = -35$ through $z = 62$, functional slice thickness = 4 mm) displaying activation significant at $\alpha = .05$ (corrected). The left image (good performers) and center image (poor performers) show one-sample *t* tests for activation related to the first ICA component. In the right image, a *t* test between good and poor performers shows greater activation for good performers (warm colors) and poor performers (cool colors). The underlying anatomical image was averaged across groups. Image displayed in radiological convention.

Behaviorally derived model. A whole brain, within-group *t* map comparing correct and error trials in good performers showed greater BOLD signal change in left inferior frontal gyrus (IFG), left MFG, and bilateral superior frontal gyrus (SFG) during error trials (Figure 4, left). Good performers also showed greater BOLD signal change in bilateral cerebellum. A whole brain, within-group *t* map comparing correct and error trials in poor performers showed greater BOLD signal change in left superior temporal gyrus and IFG during error trials (Figure 4, right).

A whole brain Group × Trial Performance interaction map showed no between-group differences on correct trials. Significant differences were observed, however, between good and poor performers on error trials $F(1,22) = 4.35$, $p = .05$ (Figure 5; see Table 1 for Talaraich coordinates). Good performers showed

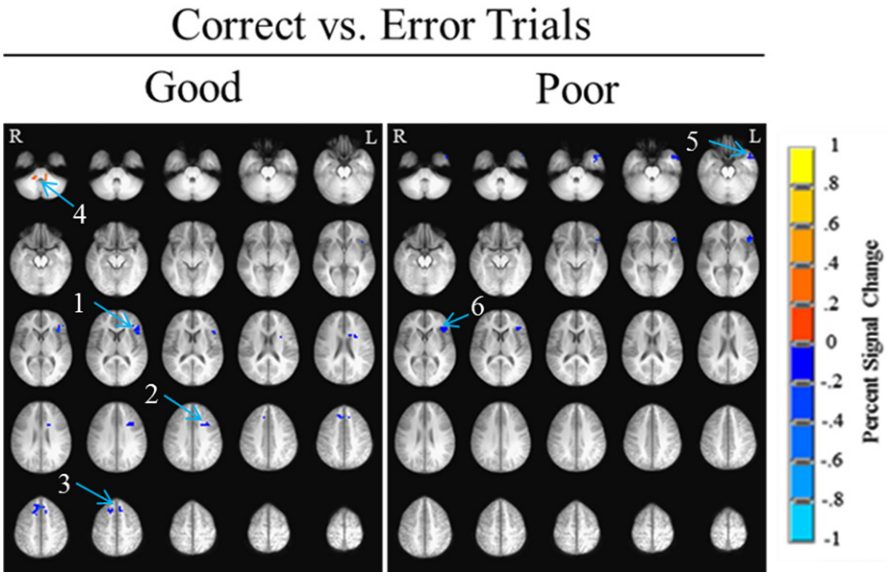

Figure 4. Within-group *t* tests. Axial slices ($z = -35$ through $z = 62$, functional slice thickness = 4 mm). The left image (good performers) and right image (poor performers) display activation significant at $\alpha = .05$ (corrected) for within-group *t* tests between correct and error trials. Cooler colors represent greater activation during error trials. Warmer colors represent greater activation during correct trials. The underlying anatomical image was averaged across groups. Image displayed in radiological convention. 1 = left inferior frontal gyrus; 2 = left middle frontal gyrus; 3 = bilateral superior frontal gyrus; 4 = bilateral cerebellum; 5 = left superior temporal gyrus; 6 = left inferior frontal gyrus.

Table 1. *Talaraich Coordinates of Significant BOLD Signal Change*

			Center of mass			
	Region	L/R	*X*	*Y*	*Z*	Cluster size (voxels)
Good vs. poor performers						
	Good > poor					
	MFG	R	40	22	36	45
	IPL	R	50	–46	33	25
		L	–54	–48	27	34
	MOG	L	–34	–70	–14	81
	Cerebellum	L	–14	–24	–24	27
	Poor > good					
	Cuneus	L	–10	–60	7	43
Error trials						
	Good > poor					
	MFG	R	39	22	23	61
	MFG	R	32	54	3	18
	IPL	R	48	–62	26	52
	Poor > good					
	Precuneus	R	13	–46	58	23
	Cerebellum	R	12	–39	–37	42

Note. MFG = middle frontal gyrus; IPL = inferior parietal lobule; MOG = middle occipital gyrus.

reduced BOLD signal change in right precuneus and right cerebellum as compared to poor performers during errors. Poor performers showed reduced BOLD signal change in two separate right MFG clusters, and in the right IPL compared to good performers during error trials.

Discussion

The main focus of this study was to elucidate the neural correlates of poor antisaccade performance in a subset of healthy young adults. The data-derived ICA analysis of overall antisaccade performance demonstrated that poor performers ($\leq 65\%$ correct) showed less BOLD signal change in regions involved in top-down cognitive control, compared to good performers ($\geq 80\%$ correct). This study also sought to dissociate activation patterns during correct trials from those during error trials through the use of trial-by-trial responses on a block design. This behaviorally derived analysis showed that good and poor performers showed similar patterns of activation on correct trials, but on error trials differential patterns of activation in MFG, IPL, precuneus, and cerebellum were observed.

Data-Derived Model

Across the blocks of antisaccade trials, both good and poor performers showed activation in SEF, FEF, PPC, PFC, MOG, striatum, and thalamus—regions which have been commonly associated with antisaccade performance (McDowell et al., 2008). Poor performers, however, showed a reduction in BOLD signal change in MFG and IPL as compared to good performers. Patterns of reduced frontal activation have been associated with deficits in saccadic inhibition in clinical populations. Patients with schizophrenia, for example, have shown decreased BOLD signal change in MFG and its associated subcortical circuitry during blocks of the antisaccade task when compared to healthy controls (McDowell et al., 2002; Tu, Yang, Kuo, Hsieh, & Su, 2006). Reduction of IPL activation among poor performers may represent a failure of sensorimotor transformation required to generate a saccade away from the cue. This is consistent with nonhuman primate neural recordings, which suggest that PPC encodes the motor signal to look away from the cue (Zhang & Barash, 2000).

Behaviorally Derived Model

Event-related designs have provided evidence for dissociating the neural correlates of correct antisaccade trials from the neural correlates of antisaccade error trials (Curtis & D'Esposito, 2003; Ettinger et al., 2008; Ford et al., 2005). In the present study, good and poor performers showed differential patterns of activation on correct and error trials. When compared within group, both good and poor performers showed greater activation in IFG during error trials. Good performers, unlike poor performers, also showed greater activation in MFG and SFG. In a Group × Trial Performance interaction, poor performers showed reduced activation compared to good performers in MFG and IPL on error, but not correct trials. These results are consistent with the Ford et al. (2005) event-related fMRI study, which provided data to suggest that a large frontal and parietal network is involved in preventing errors during the antisaccade task. Here, greater activation in frontal regions and IPL in good performers likely represents an attempt to instate cognitive control during the trial containing the antisaccade error (Clementz, Brahmbhatt, McDowell, Brown, & Sweeney, 2007; Sharpe et al., 2011). Poor performers showed similar patterns to good performers on correct trials, but showed greater activation in precuneus and cerebellum on error trials. In poor performers, greater activation in precuneus may represent an uninhibited bottom-up response to the stimuli.

The distinct patterns between good and poor performers during error trials could represent the absence of top-down prefrontal and parietal control in poor performers. Microelectrode and EEG data suggest that the PFC may send top-down inhibitory signals directly to early visual areas, ostensibly preventing saccade errors toward the stimulus (Clementz et al., 2010; Johnston & Everling, 2006; Munoz & Everling, 2004). In addition to the PFC, parietal regions have been shown to play a role in top-down modulation of visual responses. Patients with parietal lesions show an increased rate of antisaccade errors (Sharpe et al., 2011). Thus, when top-down

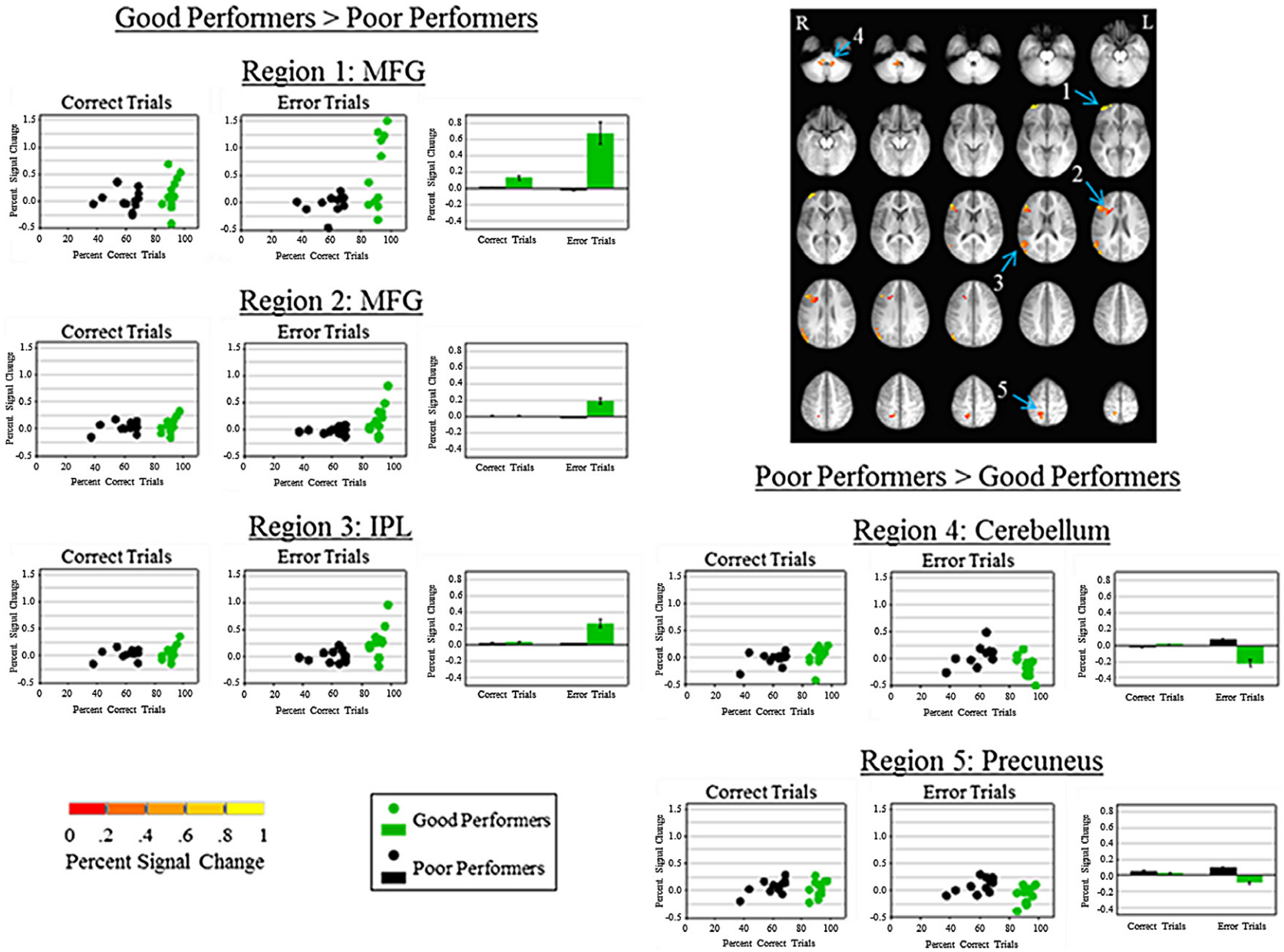

Figure 5. Group × Trial Performance interaction. Axial slices ($z = -35$ through $z = 62$, functional slice thickness = 4 mm) displaying activation significant at $\alpha = .05$ (corrected) for the group (good and poor performers) by trial performance (correct and error trials) interaction. Scatter plots show percent BOLD signal change values as a function of percent correct trials for individual good and poor performers on correct and error trials. Bar graphs display means and standard error of scatter plots. Regions 1, 2, and 3 showed greater percent BOLD signal change elicited by good performers than by poor performers on error trials. Regions 4 and 5 showed greater percent BOLD signal change elicited by poor performers than by good performers on error trials. The underlying anatomical image was averaged across groups. Image displayed in radiological convention.

control regions are not active in poor performers, bottom-up visual regions (e.g., precuneus) are uninhibited, and the likelihood of making an antisaccade error is increased. Conversely, although good performers made errors, their top-down control circuitry was more active during the errors and likely contributed to a reduced probability of a future error.

These results should be interpreted within the context of the following caveats. First, we could not assess the shape of the hemodynamic response associated with correct and error trials. Despite this, we were able to show differences in brain activation between correct and error trials. Because the hemodynamic response has been shown to be linearly additive, individual responses, such as those corresponding to correct and error trials, can be demarcated out of a block of responses, provided that they are more than 2 s apart (Dale & Buckner, 1997). Second, statistical power may have been an issue in the comparison of good and poor performers based on their correct and error trials alone. Because good performers were characterized by more correct trials, the power to predict activation due to correct trials was greater for good performers. Likewise, the power to predict activation due to error trials was greater for poor performers. This, however, did not seem to be an issue in the error trial only comparison; good performers showed greater activation in two regions, MFG and IPL, despite reduced power. Third, activation patterns in poor performers could have resulted from low task engagement, rather than deficits in cognitive control. Poor performers did, however, make correction saccades during most (89.6%) error trials. Thus, it could be argued that poor performers were engaged in the task, or else they would not have corrected error saccades.

The present findings may have potential utility for studies comparing healthy controls to patient groups. Here, we have identified a poor-performing subset of a healthy sample and shown that this group differs in terms of neural activation patterns from a group who performs well on the antisaccade task. Although sampling good-performing healthy participants is convenient, these findings suggest the importance of sampling from a full distribution of performance. Having a particularly well performing control group could bias differences in activation (Hill & Neiswanger, 1997). Thus, utilizing control groups that represent the full performance distribution for comparison with patient samples might provide further detail on circuitry specific to the illness, rather than performance.

The results from this study suggest that a failure to activate frontal and parietal regions involved in top-down control corresponds to poor antisaccade performance in healthy young adults. Moreover, these data illustrate that levels of activation in top-down control regions during error trials can differentiate cognitive control ability. Here, poor-performing healthy adults were able to activate the same top-down control regions as a good-performing subset during correct trials, but showed an absence of the activation in these regions during error trials. Therefore, future work investigating patterns of activation during error trials might help further our understanding of why people vary in their ability to instate cognitive control.

References

Beckmann, C. F., & Smith, S. M. (2004). Probabilistic independent component analysis for functional magnetic resonance imaging. *IEEE Transactions on Medical Imaging*, *23*, 137–152. doi: 10.1109/tmi.2003.822821

Clementz, B. A., Brahmbhatt, S. B., McDowell, J. E., Brown, R., & Sweeney, J. A. (2007). When does the brain inform the eyes whether and where to move? An EEG study in humans. *Cerebral Cortex, 17*, 2634–2643. doi: 10.1093/cercor/bhl171

Clementz, B. A., Gao, Y., McDowell, J. E., Moratti, S., Keedy, S. K., & Sweeney, J. A. (2010). Top-down control of visual sensory processing during an ocular motor response inhibition task. *Psychophysiology*, *47*, 1011–1018. doi: 10.1111/j.1469-8986.2010.01026.x

Connolly, J. D., Goodale, M. A., DeSouza, J. F., Menon, R. S., & Vilis, T. (2000). A comparison of frontoparietal fMRI activation during anti-saccades and anti-pointing. *Journal of Neurophysiology, 84*, 1645–55. Retrieved from http://jn.physiology.org/content/84/3/1645.full

Cox, R. W. (1996). AFNI: Software for analysis and visualization of functional magnetic resonance neuroimages. *Computers and Biomedical Research, 29*, 162–173.

Curtis, C. E., & D'Esposito, M. (2003). Success and failure suppressing reflexive behavior. *Journal of Cognitive Neuroscience, 15*, 409–418. doi: 10.1162/089892903321593126

Dale, A. M., & Buckner, R. L. (1997). Selective averaging of rapidly presented individual trials using fMRI. *Human Brain Mapping, 5*, 329–340. doi: 10.1002/(SICI)1097-0193(1997)5:5<329::AID-HBM1>3.0.CO;2-5

DeSouza, J. F., Menon, R. S., & Everling, S. (2002). Preparatory set associated with pro-saccades and anti-saccades in humans investigated with event-related fMRI. *Journal of Neurophysiology, 89*, 1016–1023. doi: 10.1152/jn.00562.2002

Dyckman, K. A., Camchong, J., Clementz, B. A., & McDowell, J. E. (2007). An effect of context on saccade-related behavior and brain activity. *NeuroImage, 36*, 774–784. doi: 10.1016/j.neuroimage.2007.03.023

Ettinger, U., Ffytche, D. H., Kumari, V., Kathmann, N., Reuter, B., Zelaya, F., & Williams, S. C. R. (2008). Decomposing the neural correlates of antisaccade eye movements using event-related fMRI. *Cerebral Cortex, 18*, 1148–1159. doi: 10.1093/cercor/bhm147

Fischer, B., Gezeck, S., & Hartnegg, K. (2000). On the production and correction of involuntary prosaccades in a gap antisaccade task. *Vision Research*, *40*, 2211–2217. doi: 10.1016%2FS0042-6989%2800%2900082-1

Ford, K. A., Goltz, H. C., Brown, M. R., & Everling, S. (2005). Neural processes associated with antisaccade performance investigated with event-related fMRI. *Journal of Neurophysiology, 94*, 429–440. doi: 10.1152/jn.00471.2004

Hallett, P. E. (1978). Primary and secondary saccades to goals defined by instructions. *Vision Research, 18*, 1279–1296. doi: 10.1016/0042-6989(78)90218-3

Hill, S. Y., & Neiswanger, K. (1997). The value of narrow psychiatric phenotypes and "super" normal controls. *Handbook of psychiatric genetics* (Vol. 236). New York, NY: CRC Press.

Hutton, S. B., & Ettinger, U. (2006). The antisaccade task as a research tool in psychopathology: A critical review. *Psychophysiology, 43*, 302–313. doi: 10.1111/j.1469-8986.2006.00403.x

Johnston, K., & Everling, S. (2006). Neural activity in monkey prefrontal cortex is modulated by task context and behavioral instruction during delayed-match-to-sample and conditional prosaccade-antisaccade tasks. *Journal of Cognitive Neuroscience, 18*, 749–765. doi: 10.1162/jocn.2006.18.5.749

Klein, C., Rauh, R., & Biscaldi, M. (2010). Cognitive correlates of antisaccade task performance. *Experimental Brain Research, 203*, 759–764. doi: 10.1007/s00221-010-2276-5

Krafft, C., Schwarz, N., Chi, L., Li, Q., Schaeffer, D., Rodrigue, A. L., . . . McDowell, J. (2012). The location and function of parietal cortex supporting of reflexive and volitional saccades, a meta-analysis of over a decade of functional MRI data. In A. Costa & E. Villalba (Eds.), *Horizons of neuroscience research, volume 9* (pp. 131–153). Hauppauge, NY: Nova Science Publishers.

Leigh, R. J., & Zee, D. S. (2006). *The neurology of eye movements* (Vol. 4). Oxford, UK: Oxford University.

Li, Q., Amlung, M. T., Valtcheva, M., Camchong, J., Austin, B. P., Dyckman, K. A., . . . McDowell, J. E. (2012). Evidence from cluster analysis for differentiation of antisaccade performance groups based on speed/accuracy trade-offs. *International Journal of Psychophysiology, 85*, 274–277. doi: 10.1016/j.ipsycho.2012.03.008

McDowell, J. E., Brown, G. G., Paulus, M., Martinez, A., Stewart, S. E., Dubowitz, D. J., & Braff, D. L. (2002). Neural correlates of refixation saccades and antisaccades in normal and schizophrenia subjects. *Biological Psychiatry, 51*, 216–223. doi: 10.1016/S0006-3223(01)01204-5

McDowell, J. E., Dyckman, K. A., Austin, B. P., & Clementz, B. A. (2008). Neurophysiology and neuroanatomy of reflexive and volitional saccades: Evidence from studies of humans. *Brain and Cognition, 68*, 255–270. doi: 10.1016/j.bandc.2008.08.016

McDowell, J. E., Kissler J. M., Berg, P., Dyckman, K. A, Gao, Y., Rockstroh, B., & Clementz, B. A. (2005). Electroencephalography/magnetoencephalography study of cortical activities preceding prosaccades and antisaccades. *NeuroReport, 16*, 663–668. doi: 10.1097/00001756-200505120-00002

McKeown, M. J. (2000). Detection of consistently task-related activations in fMRI data with hybrid independent component analysis. *NeuroImage, 11*, 24–35. doi: 10.1006/nimg.1999.0518

Munoz, D. P., & Everling, S. (2004). Look away: The anti-saccade task and the voluntary control of eye movement. *Nature Reviews Neuroscience, 5*, 218–228. doi: 10.1038/nrn1345

Sharpe, J. A., Cheng, P., & Eizenman, M. (2011). Antisaccade generation is impaired after parietal lobe lesions. *Annals of the New York Academy of Sciences, 1233*, 194–199. doi: 10.1111/j.1749-6632.2011.06178.x

Talaraich, J., & Tournoux, P. (1998). *Co-planar stereotaxic atlas of the human brain: A 3-dimensional proportional system, an approach to cerebral imaging*. New York, NY: Thieme Medical Publishers.

Tu, P., Yang, T. H., Kuo, W. J., Hsieh, J. C., & Su, T. P. (2006). Neural correlates of antisaccade deficits in schizophrenia, an fMRI study. *Journal of Psychiatric Research, 40*, 606–612. doi: 10.1016/j.jpsychires.2006.05.012

Ward, B. D. (2000). *Simultaneous inference for fMRI data, AlphaSim program documentation for AFNI*. Milwaukee, WI: Medical College of Wisconsin.

Zhang, M., & Barash, S. (2000). Neuronal switching of sensorimotor transformations for antisaccades. *Nature, 408*, 971–975. doi: 10.1038/35050097

(Received August 30, 2012; Accepted December 18, 2012)